

**Oxford Instruments Plasma Technology**  
North End, Yatton, Bristol BS49 4AP, UK

Tel: +44 (0) 1934 837000  
Fax: +44 (0) 1934 837001  
Email: [plasma@oxinst.com](mailto:plasma@oxinst.com)  
[www.oxford-instruments.com](http://www.oxford-instruments.com)

## Growth of platinum films by atomic layer deposition (ALD)

*Dr. Qi Fang*

Oxford Instruments Plasma Technology

### Abstract

This white paper details both the remote-plasma and thermal-ALD processing utilised in the deposition of platinum films. Platinum films were grown on Si wafers, SiO<sub>2</sub>, Al<sub>2</sub>O<sub>3</sub> and high-k dielectric HfO<sub>2</sub> ALD films on Si substrates at 300°C, using methylcyclopentadienyl trimethyl platinum (MeCpPtMe<sub>3</sub>) and O<sub>2</sub> as precursors. The ALD Pt-films deposited were homogeneous and resulted in a low resistivity of 12.8 μΩ-cm. AES studies revealed high quality Pt films deposited by both thermal and plasma ALD with carbon impurity less than 1.5% and oxygen found only in the interface. SEM and EDX were used to investigate Pt nucleation and growth in ALD processes. It is remarkable that the nucleation delay of between thermal and plasma ALD Pt was different though they are a similar growth rate of 0.45 Å/cycle. In this paper, the Pt ALD nucleation and growth behaviours with precursor dose times, O<sub>2</sub> or O<sub>2</sub> plasma exposures and substrates are also described.

### 1 Introduction

Ultrathin metallic layers such as Pt, Ru, Pd and Cu deposited onto oxide structural surfaces have wide applications in microelectronics, catalysis, photonics and chemical sensing [1-4]. Platinum films have a large variety of potential applications in nanotechnology, microelectronics and energy technologies due to their chemical stability, catalytic activity, and excellent electronic properties [5-7]. During the past decade atomic layer deposition (ALD) as an outstanding technique of self-limiting and thickness accurately controlling, is used to fabricate ultrathin and conformal thin film structures for many potential applications in advanced high dielectric constant (high-k) gate oxides, electrode and connection materials, storage capacitor dielectrics and copper diffusion barriers in advanced electronic devices, as well as for solar energy and biological applications [8, 9]. A unique attribution of ALD is that it uses sequential self-limiting surface reactions to achieve control of film growth in the monolayer or sub-monolayer thickness regime. Therefore, ALD is receiving wide attention for the ultrathin layers grown on to micro- and nano-devices with three-dimension in a high aspect ratio. Furthermore, ALD can also be used for any advanced technologies that require control of film structure in the nanometer or sub-nanometer scale due to its capacity for self-terminating conformal layer formation.

The most of publishes of Pt ALD processes reported are used the thermal ALD process using methylcyclopentadienyl trimethylplatinum (MeCpPtMe<sub>3</sub>) and O<sub>2</sub> gas [10-12]. This process is based on the dissociative chemisorption of O<sub>2</sub> on the Pt surface for oxidative decomposition of the precursor ligands [13]. However, this oxidative decomposition becomes extremely difficult in the initial stage (without Pt nano-particle to be formed yet) of a thermal ALD process, leading to a nucleation delay. Knoops and his co-authors reported the Pt and PtO<sub>2</sub> processes by using both remote plasma ALD and the thermal ALD of Pt. Their work shows that the remote plasma process leads to immediate growth without substantial nucleation delay, while the thermal ALD process leads to no growth at all unless a Pt starting surface or a high O<sub>2</sub> pressure is employed [1]. In the O<sub>2</sub> plasma, O radicals are created, providing atomic O to the surface directly from the gas phase, enhancing oxygen chemisorption on the surface and oxidation of the precursor ligands. [14]

However, despite its successful Pt depositions, the ALD process lacks a detailed atomic-scale understanding of the formed interface structure and the effect of substrate used on the Pt growth, which is extremely important for microelectronic applications. In this work, platinum films were grown on Si wafers, SiO<sub>2</sub>, Al<sub>2</sub>O<sub>3</sub> and high-k dielectric HfO<sub>2</sub> ALD films on Si substrates by both remote plasma and thermal atomic layer deposition (ALD), using methylcyclopentadienyl trimethyl platinum (MeCpPtMe<sub>3</sub>) and O<sub>2</sub> as precursors. The Pt ALD growth behaviours with precursor dose times, O<sub>2</sub> or O<sub>2</sub> plasma exposures and substrates are investigated. Furthermore, the Pt ALD process on various oxide substrates, Pt nucleation process, electrical property and chemical impurities of the Pt thin film are also discussed.

## 2 Experimental

The Pt films were deposited in an ALD system with load-lock delivery (FlexAL-MK II, Oxford Instruments Plasma Technology). The deposition system was connected to an inductively coupled plasma (ICP) source and in-situ ellipsometer, which can perform both of remote plasma ALD and thermal ALD capabilities within a single system.

The pump unit consisted of a turbo molecular pump and a dry pump reaching a base pressure of  $1 \times 10^{-6}$  mbar. Trimethyl (methylcyclopentadienyl) platinum(IV) ( $\text{MeCpPtMe}_3$ ) (SAFC, Sigma-Aldrich) in a stainless steel bubbler, heated to  $70^\circ\text{C}$ , was used as Pt- precursor and vapor drawn into the chamber.

The process of Pt films carried out by both thermal and remote  $\text{O}_2$ -plasma ALD at  $300^\circ\text{C}$ , using methylcyclopentadienyl trimethyl platinum ( $\text{MeCpPtMe}_3$ ) and  $\text{O}_2$  as precursors. The  $\text{MeCpPtMe}_3$  precursor was vaporized at  $70^\circ\text{C}$  using the vapour-draw method without bubbling gas and using 200sccm of Ar gas flow as purge gas. To maximise precursor usage, the first half-cycle consisted of  $\text{MeCpPtMe}_3$  precursor dosing with the bottom valve closed (no pumping) a holding for 5-10 seconds, in the process investigation. Si (100) with native oxide layer was used as the substrate. For the oxide samples, Si (100) substrates were first coated prior to the Pt metal ALD with 10-20 nm of ALD  $\text{Al}_2\text{O}_3$ ,  $\text{HfO}_2$  and  $\text{SiO}_2$  using alternating ALD processes of TMA(trimethylaluminium)/ $\text{O}_2$ -plasma, TEMAH [Tetrakis(ethylmethylamino) hafnium]/ $\text{O}_2$ -plasma and TRDMAS [tris(dimethylamino) silane]/ $\text{O}_2$ -plasma, respectively. Table 1 shows the details of the four types of substrates used, namely: Si wafers,  $\text{SiO}_2$ ,  $\text{Al}_2\text{O}_3$  and high-k dielectric  $\text{HfO}_2$  ALD films on Si substrates.



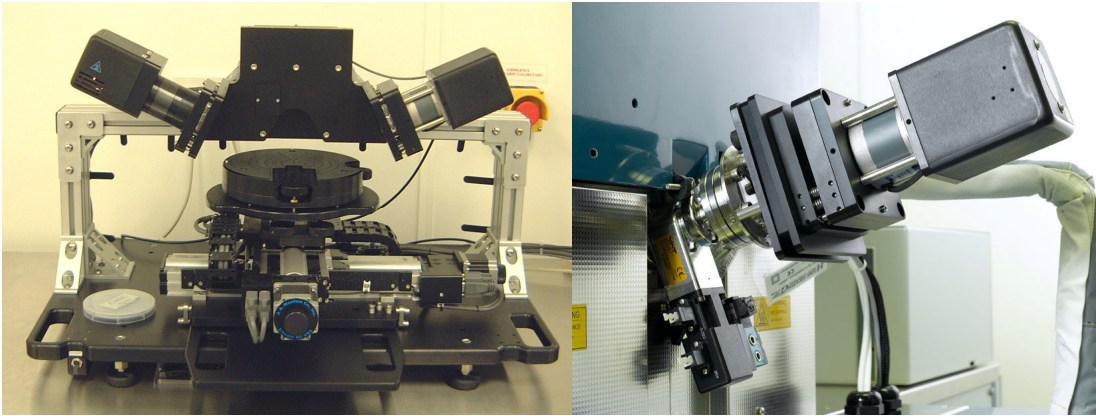
*FlexAL-MK II, Oxford Instruments Plasma Technology*

**Table 1, the substrates used for ALD-Pt film deposition**

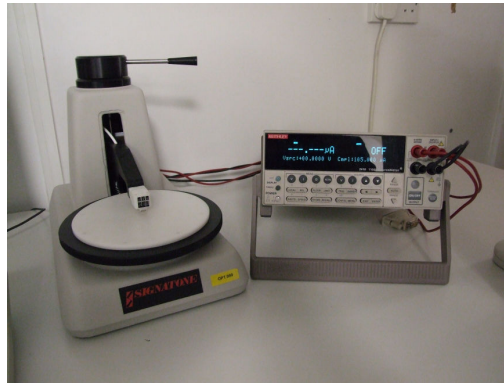
Substrate	ALD-oxide process	ALD oxide film thickness (nm)	ALD process temperature ( $^\circ\text{C}$ )	ALD precursors
Si(100)	/	/	/	/
$\text{SiO}_2/\text{Si}$	Plasma-ALD	10	200	TRDMAS
$\text{Al}_2\text{O}_3/\text{Si}$	Plasma-ALD	18	200	TMA
$\text{HfO}_2/\text{Si}$	Plasma-ALD	10	290	TEMAH

ALD chamber pressure was varied from 10 to 40 millitorr during the process steps. Not only the wafer holder stage was heated but also the chamber wall and delivery line were heated to a temperature of  $120^\circ\text{C}$  and  $80^\circ\text{C}$ , respectively, to prevent the precursor condensation and make the sample surface temperature the same. The remote  $\text{O}_2$  plasma was generated by a radio frequency (rf) induction-type plasma generator (ICP). The plasma power was 300 W.

The thickness and the refractive index of the ALD films were measured using a J.A. Woollam M2000V spectroscopic ellipsometer (370nm-1000nm wavelengths) and also confirmed by cross sectional SEM (Zeiss, SUPRA-25). Energy dispersive X-ray (EDX) (INCA-7426, Oxford Instruments) and Auger Electron Spectroscopy (AES) were used for determining the chemical composition and element profile of the ALD films. A 4-point probe (Signatone 4 point probe with a Keithley 2410 Source) was applied for testing the electrical property of the film.



Left: Ex-situ M2000 ellipsometer with motorized X-Y mapping stage at Oxford Instruments. Right: the M2000 ellipsometer mounted in-situ on the FlexAL tool in OIPT's laboratory.



Signatone 4-point probe connected to a Keithley 2410 Source meter

### 3 Results and discussions

#### 3.1 Platinum ALD

##### 3.1.1 Platinum by thermal-ALD

Figure 1 shows the growth rate and resistivity of platinum films by thermal-ALD against the precursor dose-time for 600 cycles at 300°C. The growth rate of 0.45-0.47 Å/cycle and the resistivity of platinum films of about 13.5μΩ-cm from 600 cycles were obtained.

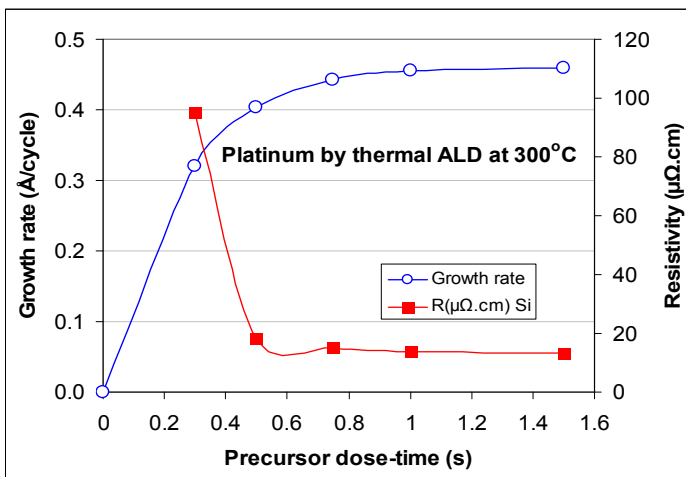
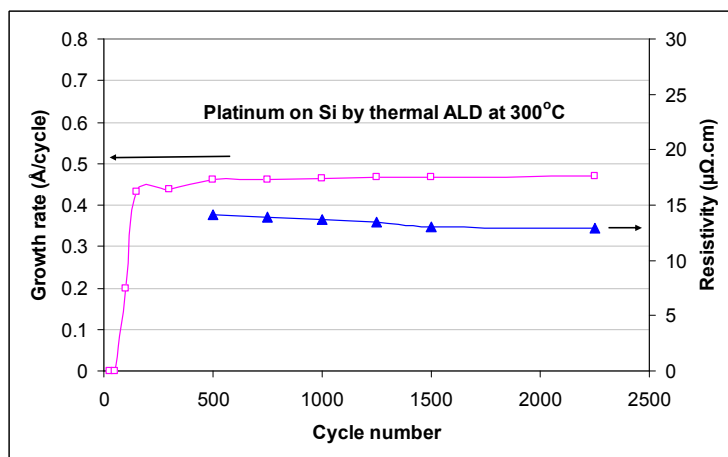


Figure 1, growth rate and resistivity of platinum films by thermal-ALD at 300°C vs precursor dose-time for 600 cycles



To confirm the growth rate and to investigate the relationship of resistivity and film thickness of the platinum films by thermal-ALD, Figure 2 gives the growth rate (GR) and resistivity of platinum films using ALD cycle numbers up to 2250. It is found that GR of Pt increases slightly for long deposition, but is still around 0.45-0.475 Å/cycle. The resistivity of Pt films are in a range of 14.1 to 12.8 μΩ·cm from 500 to 2250 cycles and the resistivity of the Pt layer on Si was found to be slightly reduced with increasing Pt thickness, the lowest resistivity of 12.8 μΩ·cm were measured with a Pt thickness of 100 nm on Si substrates. SEM was used to investigate Pt nucleation and growth in ALD processes.



**Figure 2**, growth rate (GR) and resistivity of platinum films by thermal-ALD vs cycle number and it is found that a GR of Pt thermal-ALD is around 0.45-0.475 Å/cycle and the resistivity range of 14.1 to 12.8 μΩ·cm from 500 cycle to 2250 cycle.

The nucleation delay in thermal ALD of Pt was found at about 70 cycles from figure 3, which has been confirmed by SEM observations.

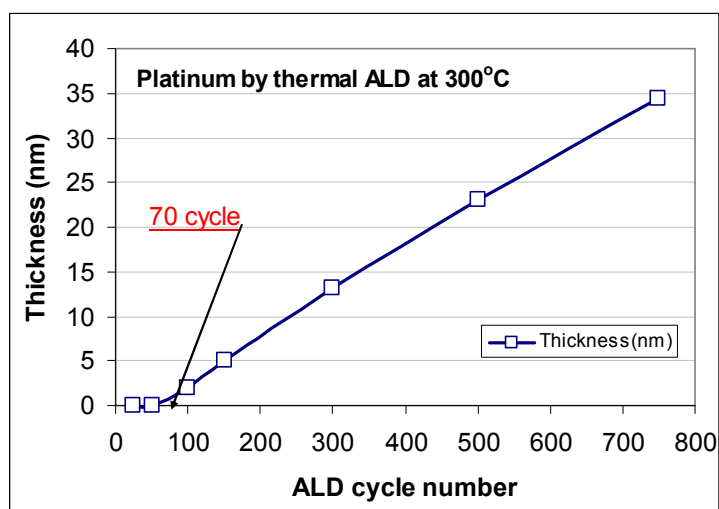


**Figure 3**, thickness of platinum films by thermal-ALD vs cycle number at 300°C and the nucleation delay of Pt thermal-ALD to be found is around 70 cycles.

Elam reported the nucleation behaviors of Pd and Pt on various substrates. [15, 16] They found that the Pt films deposited concurrently on Si (100) substrates showed Pt particles that increase in size with the number of Pt ALD cycles performed such that the Pt film is nearly continuous after 75-100 cycles. [16]

### 3.1.2 Platinum by plasma-ALD

Figure 4 shows the growth rate of platinum films by plasma-ALD against precursor dose-time at 300°C. The growth rates of 0.43-0.45 Å/cycle were obtained, which is comparable to that of thermal ALD.

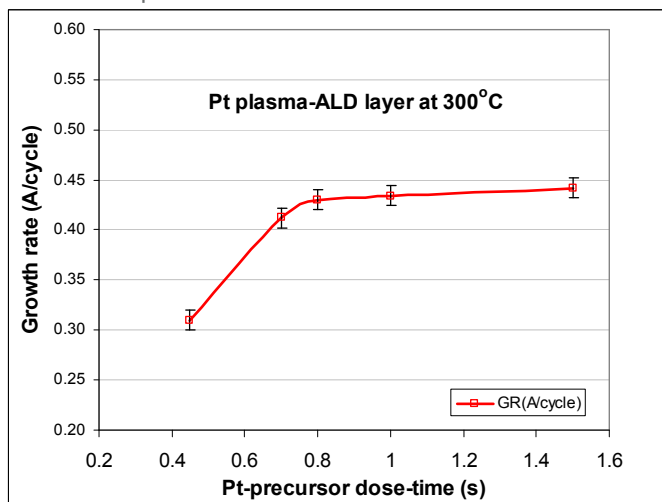


Figure 4, growth rate of platinum films by plasma-ALD at 300°C vs precursor dose-time

The thickness and resistivity of platinum films by plasma-ALD with cycle number at 300°C are shown Figure 5. The resistivity of the platinum films is below 14.5  $\mu\Omega\cdot\text{cm}$  after plasma ALD of 500 cycles and the nucleation delay of Pt plasma-ALD is around 20 cycles. Comparing to the nucleation delay of Pt thermal-ALD of 70 cycles, it shows that plasma-ALD can reduce the nucleation delay of Pt. The remote plasma enhanced ALD Pt films showed a short nucleation delay on all the different types of substrates, and an active nucleation behaviour which resulted in a very smooth film surface morphology.

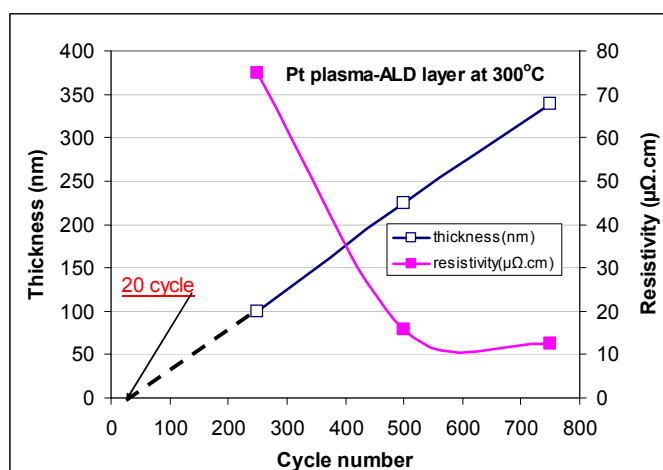


Figure 5, thickness and resistivity of platinum films by plasma-ALD vs cycle number at 300°C and the nucleation delay of Pt plasma-ALD is around 20 cycles. Comparing to the nucleation delay of Pt thermal-ALD of 70 cycles, it shows that plasma-ALD can reduce the nucleation delay of Pt.

The resistivity of platinum films on various oxides by plasma-ALD at 300°C against precursor dose-time is shown in Figure 6. The resistivity of the Pt layers was found to be reduced with increasing precursor dose up to 1.5s and the lowest resistivity of Pt was found on  $\text{HfO}_2$ . It is clear that the resistivity of Pt film grown on oxides is  $\text{Si/SiO}_2 > \text{Si/Al}_2\text{O}_3 > \text{Si/HfO}_2$ .

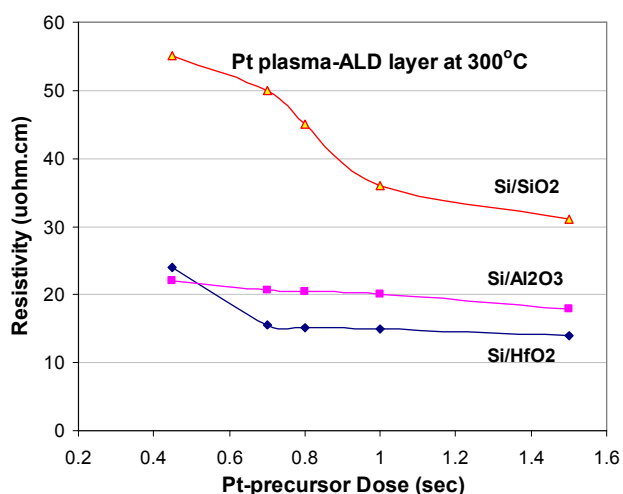


Figure 6, resistivity of platinum film on various oxides by plasma-ALD at 300°C vs precursor dose-time. It is clear that the order of resistivity of Pt film grown on oxides is  $Si/SiO_2 > Si/Al_2O_3 > Si/HfO_2$

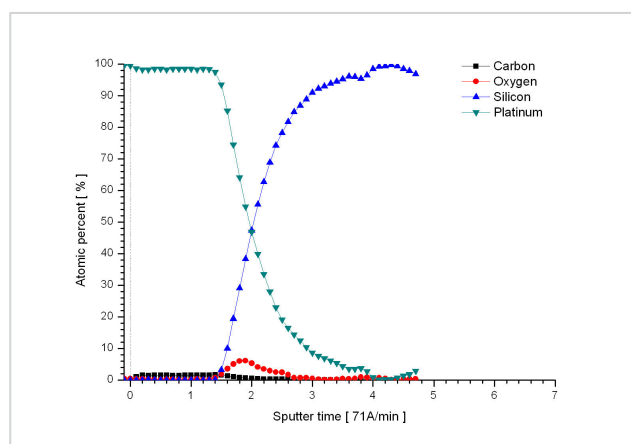


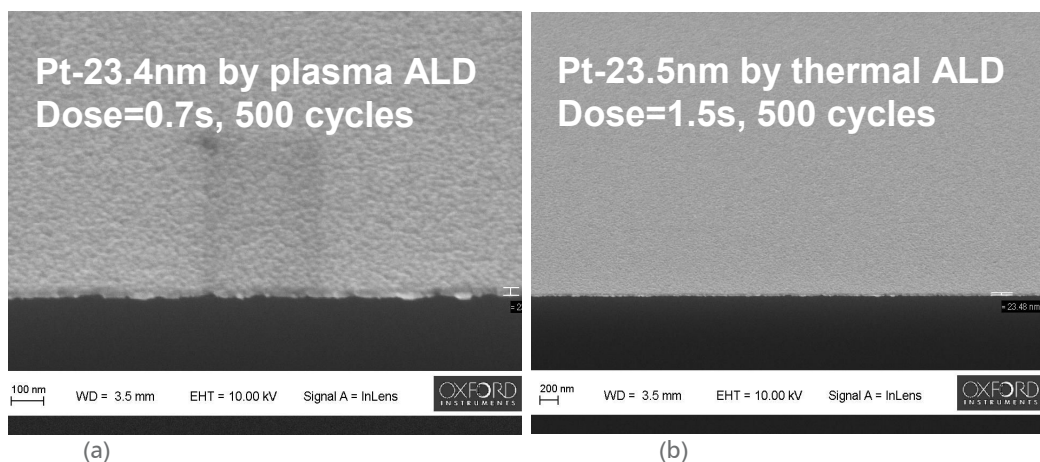
Figure 7, AES of 30nm Pt film grown by plasma-ALD.

AES profile scanning and EDX testing were applied for the elemental analysis in the film and interfaces. AES studies revealed high quality Pt films deposited by both thermal and plasma ALD with carbon impurity less than 1.5% and oxygen found only in the interface (Fig.7).

### 3.1.3 Platinum nano-particle islands and nucleation delay

Our initial Pt thermal ALD experiments on Si surfaces revealed nucleation and growth behaviour of forming Pt nano-particle islands. Figure 8(a) and 8(b) show a similar SEM cross-section thickness of Pt-ALD films grown by using plasma and thermal ALD for 500 cycles at 300°C. The particle-size measurement was based on SEM and SE. One example of average Pt-size of 5.5 nm grown on Si by thermal ALD for 150 cycles at 300°C is shown in Figure 8(d). The detailed measurements showed that the average nano-particle island size of Pt grown on Si by plasma ALD is bigger than that of thermal ALD at same cycle numbers.

Table 2 gives a short summary of Pt particle-size at 50 and 100 cycles, respectively, and the process data of Pt films on the surface of Si, SiO<sub>2</sub>, Al<sub>2</sub>O<sub>3</sub> and HfO<sub>2</sub> deposited at 300°C by thermal and remote plasma ALD for 500 cycles. The growth rate and resistivity of Pt plasma-ALD layers on various oxides is shown in Figure 9. HfO<sub>2</sub> is shown the highest growth rate and the lowest resistivity of them. It is believed that surface functionalisation by plasma-ALD and rich-absorbed oxygen radicals on HfO<sub>2</sub> surface are the reasons.



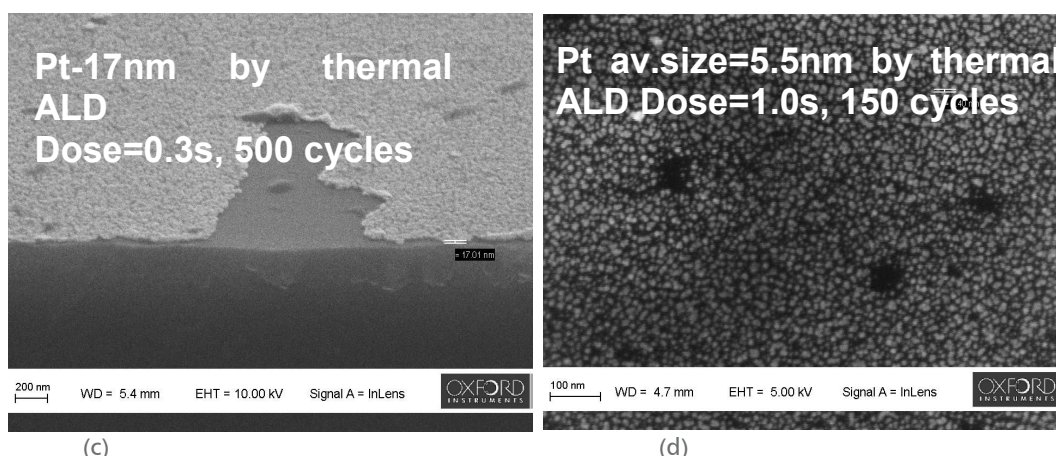


Figure 8, SEM of Pt-ALD films (cross-section of thickness and particle-size measurement).

Table 2, the process data of Pt films on the surface of Si, SiO<sub>2</sub>, Al<sub>2</sub>O<sub>3</sub> and HfO<sub>2</sub> deposited at 300°C by thermal and remote plasma ALD using MeCpPtMe<sub>3</sub> and O<sub>2</sub> gas or O<sub>2</sub> plasma (500 cycles)

Pt-sample runs	ALD process	Substrate	Particle size at 50 cycles	Particle size At 100 cycles	Growth rate (Å/cycle)	Resistivity (μΩ-cm)
1	Thermal-ALD	Si/native SiO <sub>2</sub> (~1nm)	1.6 ± 0.2	2.1 ± 0.2	0.44 ± 0.01	14.1 ± 0.2
2	Plasma-ALD	Si/native SiO <sub>2</sub> (~1nm)	2.0 ± 0.2	3.2 ± 0.2	0.45 ± 0.01	14.5 ± 0.2
3	Thermal-ALD	Si/SiO <sub>2</sub> (10nm ALD)	2.2 ± 0.2	2.6 ± 0.2	0.43 ± 0.01	15.1 ± 0.2
4	Plasma-ALD	Si/SiO <sub>2</sub> (10nm ALD)	2.5 ± 0.2	3.6 ± 0.2	0.44 ± 0.01	31.2 ± 0.5
5	Thermal-ALD	Si/Al <sub>2</sub> O <sub>3</sub> (18nm ALD)	/	/	0.46 ± 0.01	25.2 ± 0.5
6	Plasma-ALD	Si/Al <sub>2</sub> O <sub>3</sub> (18nm ALD)	/	/	0.47 ± 0.02	18.3 ± 0.3
7	Plasma-ALD	Si/HfO <sub>2</sub> (10nm ALD)	3.7 ± 0.3	5.6 ± 0.5	0.49 ± 0.02	14.0 ± 0.5

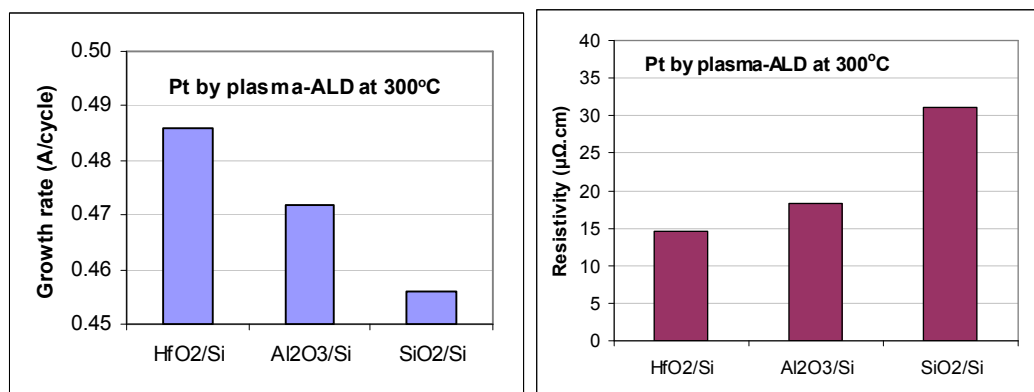


Figure 9, Growth rate and resistivity of Pt plasma-ALD layers on various oxides. HfO<sub>2</sub> is shown the highest growth rate and the lowest resistivity of them. It is believed that surface functionasation by plasma-ALD and rich-absorbed oxygen radicals on HfO<sub>2</sub> surface are the reasons.

From Fig.3 and Fig.5 we have found that the Pt films deposited on Si (100) substrates showed a Pt nucleation delay of 70 cycles and 20 cycles grown by thermal ALD and plasma-ALD before the Pt ALD process goes to a linear growth. Table 2 shows Pt particles increase in size with the number of Pt ALD cycles performed and it is also clear that the Pt particles grown by plasma-ALD is bigger than that by thermal ALD. It is believed that surface functionasation by plasma-ALD plays a important role to short the nucleation delay. In the O<sub>2</sub> plasma, O radicals are created, leading to three effects on the Pt-growth by reducing the nucleation delay: 1) providing active atomic O to the surface; 2) increasing oxidation with the ligands of the chemisorbed precursor on the surface; and 3) increasing Pt nucleation by extra plasma energy.

Pt particle-size at 50 and 100 cycles on different metal oxide surfaces ( $\text{SiO}_2$ ,  $\text{Al}_2\text{O}_3$  and  $\text{HfO}_2$ ) deposited at  $300^\circ\text{C}$  by thermal and remote plasma ALD also is shown in Table 2. It was found that the Pt particle-size on  $\text{HfO}_2$  was quite big, 3.7 nm for 50 cycles and 5.6 nm for 100 cycles as compared to 1.6 nm and 2.1 nm on Si, respectively.

Studies found that high work function metals such as Pt show instability in oxygen-deficient conditions. [19] As well known, Pt ALD process relies on the dissociative chemisorption of  $\text{O}_2$  on the Pt surface for oxidative decomposition of the precursor ligands. [17, 18] Therefore the absorbed oxygen on surface of oxides might be a controlling step for the initial step of the Pt ALD process. Considering Fermi level pinning in terms of oxygen vacancies, these appear to exist in sizable amounts in  $\text{HfO}_2$  film, [20] which is named high temperature oxygen ion conductor and allows oxygen transport across the  $\text{HfO}_2$  layer. [21, 22] The remote plasma enhanced ALD Pt films showed bigger Pt particle-size and a short nucleation delay on  $\text{HfO}_2$  films. Both active atomic O species generated from oxygen plasma and their absorption and diffusion on the  $\text{HfO}_2$  surface resulted in increasing growth rate of Pt layer on the  $\text{HfO}_2$  by plasma-ALD.

#### 4 Conclusions

Platinum films were deposited by both remote plasma and thermal atomic layer deposition (ALD) using methylcyclopentadienyl-trimethyl platinum ( $\text{MeCpPtMe}_3$ ) and  $\text{O}_2$  as precursors on oxide materials. The ALD Pt-films deposited were homogeneous and resulted in a low resistivity of  $12.8 \mu\Omega\text{-cm}$ .

AES studies revealed high quality Pt films deposited by both thermal and plasma ALD with carbon impurity less than 1.5% and oxygen found only in the interface. SEM and EDX investigations of Pt nucleation and growth in ALD processes showed that the plasma ALD can form bigger size Pt particles in the early stage and reduce the nucleation delay. Pt on  $\text{HfO}_2$  is shown the highest growth rate and the lowest resistivity of the oxides. It is believed that surface functionalisation by plasma-ALD and rich-absorbed oxygen radicals on  $\text{HfO}_2$  surface are the reasons. In the  $\text{O}_2$  plasma, O radicals are created, leading to three effects on the Pt-growth by reducing the nucleation delay: 1) providing active atomic O to the surface; 2) increasing oxidation with the ligands of the chemisorbed precursor on the surface; and 3) increasing Pt nucleation by extra plasma energy.

#### References:

1. H. C. M. Knoop, A. J. M. Mackus, M. E. Donders, M. C. M. van de Sanden, P. H. L. Notten and W. M. M. Kessels, *Electrochemical and Solid-State Letters*, **12** (7) G34-G36 (2009).
2. J. J. Senkevich, F. Tang, D. Rogers and T. M. Lu, *Chemical Vapour Deposition*, **9** (5) 258-264 (2003)
3. Seong Keun Kim, Sang Young Lee, Sang Woon Lee, Gyu Weon Hwang, Cheol Seong Hwang, Jin Wook Lee, and Jaehack Jeong, *Journal of The Electrochemical Society*, **154** (2) D95-D101 (2007).
4. Zhengwen Li, Roy G. Gordon, a, Damon B. Farmer, Youbo Lin and Joost Vlassak, *Electrochemical and Solid-State Letters*, **8** (7) G182-G185 (2005).
5. M. Armand and J. M. Tarascon, *Nature (London)*, **451**, 652 (2008).
6. L. Baggetto, R. A. H. Niessen, F. Roozeboom, and P. H. L. Notten, *Adv. Funct. Mater.*, **18**, 1057 (2008).
7. R. R. Hoover and Y. V. Tolmachev, *J. Electrochem. Soc.*, **156**, A37 (2009).
8. S.B.S. Heil, J.L. van Hemmen, C.J. Hodson, N. Singh, J.H. Klootwijk, F. Roozeboom, M.C.M. van de Sanden and W.M.M. Kessels, *J. Vac. Sci. Technol. A*, 1357, (2007).
9. Steven M. George, *Chem. Rev.*, **110**, 111-131(2010).
10. Titta Aaltonen, Mikko Ritala, Timo Sajavaara, Juhani Keinonen, and Markku Leskelä, *Chem. Mater.*, **15** (9), 1924-1928(2003)
11. Y. Zhu, K. A. Dunn, and A. E. Kaloyeros, *J. Mater. Res.*, **22**, 1292 (2007).
12. X. Jiang and S. F. Bent, *J. Electrochem. Soc.*, **154**, D648 (2007).
13. T. Aaltonen, A. Rahtu, M. Ritala, and M. Leskelä, *Electrochem. Solid-State Lett.*, **6**, C130 (2003).
14. J. F. Weaver, J. J. Chen, and A. L. Gerrard, *Surf. Sci.*, **592**, 83 (2005).
15. J. W. Elam, A. Zinovev, C. Y. Han, H. H. Wang, U. Welp, H. J. N and P. M. J, *Thin Solid Films*, **515**, 1664, (2006).
16. J. W. Elam, A. V. Zinovev, M. J. Pellin, D. J. Comstock, and M. C. Hersam, *ECS Transactions*, **3** (15) 271-278 (2007)
17. T. Aaltonen, A. Rahtu, M. Ritala, and M. Leskelä, *Electrochem. Solid-State Lett.*, **6**, C130 (2003).
18. C. T. Campbell, G. Ertl, H. Kuipers, and J. Segner, *Surf. Sci.*, **107**, 220 (1981).
19. J. K. Schaeffer, L. Fonseca, S. Samavedam, D. C. Gilmer, Y. Liang, S. Kalpat, H. H. Tseng, Y. Shiho, A. Demkov, R. Hegde, W. Taylor, D. Triyoso, D. Roan, B. White, and P. Tobin, *Appl. Phys. Lett.* **85**, 1826 (2004).
20. S. Walsh, L. Fang, J. K. Schaeffer, E. Weisbrod, and L. J. Brillson, *Appl. Phys. Lett.* **90** 052901 (2007).
21. S. Guha and V. Narayanan, *Phys. Rev. Lett.* **98** 196101 (2007).
22. R. P. Pezzi, M. Copel, M. Gordon, E. Cartier, and I. J. R. Baumvol, *Appl. Phys. Lett.* **88** 243509 (2006).

